Journal of Applied Polymer Science

Preparation of Zn Porphyrin-Functionalized Polystyrene and the Fluorescence Quenching of It by Terbuthylazine

Ruixin Wang, Baojiao Gao, Weizhou Jiao, Long Yu, Wen Pan
Department of Chemical Engineering, North University of China, Taiyuan 030051, People's Republic of China
Correspondence to: R. Wang (E-mail: wrx0212@126.com)

ABSTRACT: Zinc tetraphenylporphyrin (ZnPP) was bond on the side chains of linear chloromethylated polystyrene (CMPS) through Friedel–Crafts alkylation reaction, and the metalloporphyrin-functionalized polystyrene (ZnPP/PS) was obtained successfully. Its chemical structure was characterized with FTIR. And the effects of various factors on the bonding reaction of ZnPP had been investigated in detail. In addition, the photophysical properties of ZnPP/PS were studied by means of UV-Vis spectroscopy and fluorescence spectroscopy. The research results show that ZnPP/PS could be prepared favorably through Friedel–Crafts alkylation reaction between ZnPP and CMPS, and the most bonding degree of ZnPP on PS is up to 7% under the condition of the temperature 25°C and 0.1 mL of $SnCl_4$ lasting 8 h. Moreover, ZnPP/PS show the characteristic photophysical behavior similar to ZnPP. ZnPP moieties in ZnPP/PS interact with terbuthylazine (TBA) and form a complex with a red-shift of Q-band of absorbance peak from 559 to 565 nm. Especially TBA quenches ZnPP/PS emission intensity at 610 and 662 nm when excites at 423 nm. The TBA-ZnPP/PS complex is formed in the ground state and TBA is bonded to the excited state of ZnPP/PS simultaneously on the basis of a non-linear Stern–Volmer plot indicative of the combined dynamic and static quenching. © 2014 Wiley Periodicals, Inc. J. Appl. Polym. Sci. **2014**, *131*, 40516.

KEYWORDS: bonding; fluorescence quenching; polystyrene; terbuthylazine; zinc porphyrin

Received 16 November 2013; accepted 25 January 2014
DOI: 10.1002/app.40516

INTRODUCTION

Triazine herbicides are well-known herbicides that are widely used for annual and perennial grass and absorbed by the roots of seedling weeds. Triazine and its degradation products may be dangerous for human health because they are suspected to cause cancers, birth defects, and interruption of hormone functions, and are usually reportedly present in waters, soils, and organisms due to their high persistency.[1–3] Thus monitoring of content of these compounds in soil, water, and food chains is necessary to estimate the human exposure to these substances, and a number of technologies have been developed for their detection including Gas Chromatography (GC), Gas Chromatography/MassSpectrometry (GC/MS), High Performance Liquid Chromatography (HPLC), Liquid Chromatography/MassSpectrometry (LC/MS) and so on.[4–7] Nevertheless, these methods have some shortcomings, such as complex sample pretreatment, the valuable equipment carried difficultly, the more sample, etc. So some new detection technologies for triazine herbicides are requested like electrochemical and photochemical detection having been developed for other herbicides,[8,9] which must be more sensitive, quick, accurate, and convenient comparing with traditional methods.

Chemosensors have attracted increasing interest for detecting various organic compounds in recent years, in which fluorescent sensors have been paid more attention due to its high sensitivity and good selectivity.[10,11] Porphyrins have unique biological activity and excellent physicochemical property as a result of their characteristic ring structure of conjugated double bonds, and have been widely used in many fields, such as sensors, solar cells, photodynamic therapy, and so forth.[12–16] In especial, the porphyrin chromophore is one of the most promising signaling units for constructing fluorescent sensors due to its advantageous photophysical features,[17,18] such as pronounced photostability, high extinction coefficient, larger stokes shift, relatively long excitation wavelength (>400 nm) and emission wavelength (>600 nm), high fluorescence quantum yields (up to 0.2), and tunable fluorescence emission. In addition, the spectrophotometric characteristics of porphyrin could be altered by the bonding or interaction with other molecules and ions, and the greater the association energy and association constant, the greater the spectra change,[19,20] which is essential for forming the basis of optical sensor elements. Recently a considerable stack of reports have been published on the usage of porphyrins and its derivatives in sensors for detecting toxic gases, metal ions, herbicides, and so forth.[21,22]

Zn (II) porphyrins are of particular interest in sensor development, as these chromophores exhibit significant fluorescence quantum yields and can interact with a wide variety of axial ligands composed of nitrogenous bases through the Zn (II) ion.[23,24] Moreover, the feature spectrum of Zn (II) porphyrin exhibits good sensitivity and selectivity toward nitrogen- and oxygen-containing compounds and other small molecules and ions. As shown in our articles,[25,26] the electronic absorption and fluorescence spectra of Zn (II) porphyrins change for interacting with axial ligands including pyridine and imidazole. All of these above allow these chromophores to be examined as sensor platforms for detection of nitrogenous compounds. However, some drawbacks of the free porphyrins and their metal complexes in various applications are pointed out, for example, weak chemical stability, poor processability, concentration quenching, and the inferior mechanical property resulted by doping porphyrins. A superior strategy to overcome the above problems is to bind them to various solid supports, including silica, polymer, hybrid materials, and others.[27–30]

In this work, the free zinc tetraphenylporphyrin (ZnPP) was bond on the side group of polystyrene (PS) through the macromolecule reaction, resulting in the metalloporphyrin-functionalized polymers ZnPP/PS, so as to remove shortcomings of the free ZnPP. In addition, we investigated the spectral properties of ZnPP/PS, especially the sensitivity of fluorescence spectrum of ZnPP/PS exposed to terbuthylazine molecules, and had acquired good results, i.e., ZnPP/PS presented good optical properties, and the efficient quenching of ZnPP/PS by terbuthylazine was showed. This study will be helpful in providing a greater understanding of bonding metalloporphyrins (MPs) onto polymers depending on the covalent binding between supports and porphyrins, and in application of MPs in fluorescent chemosensors for detecting terbuthylazine.

EXPERIMENTAL

Materials and Instruments

PS ($\bar{M}_r = 8\times10^4$, Sinopec Beijing Yanshan Company, Beijing, China) was of industrial grade; Chloromethylated polystyrene (CMPS) was self-synthesized,[31] and its content of chlorine was 15% (mass percentage); tetraphenylporphyrin (TPP) and ZnPP were self-synthesized with Alder method according to the literature[30]; other chemicals were of analytical grade.

The instruments used in this study were as follows: PerkinElmer 1700 infrared spectrometer (IR, PerkinElmer Company), Thermo SOLAAR atomic absorption spectrometer (AAS, Thermo Company), Unic UV/Vis-2602 spectrophotometer (Unic Company); Hitachi F-2500 fluorescence spectrometer (Hitachi Company, Japan).

Preparation of Metalloporphyrin-Functionalized Polystyrene

CMPS and ZnPP were used as starting substances to prepare ZnPP/PS. About 0.25 g of CMPS and a certain amount of N,N′-dimethyl formamide (DMF) were added into a four-necked flask of 100 mL, and the polymer was dissolved. Then ZnPP with 1.2 times the mole number of CH_2Cl groups in CMPS dissolved in DMF was introduced, following the addition of $SnCl_4$ into it. The bonding reaction of ZnPP onto CMPS was performed at certain temperature with stirring for 8 h. After ending the reaction, the product polymer in lavender, namely ZnPP/PS, was precipitated with ethanol as precipitator, washed repeatedly with $CHCl_3$ and DMF until there was no ZnPP in the filtrate by UV detection, and dried. The structure of product was characterized with FTIR and ^{1}H-NMR. The data of ^{1}H-NMR spectrum are as follows: the peaks at 7.652, 7.674, and 7.693 ppm (meta-H and papa-H of benzene rings), the peaks at 8.155 and 8.172 ppm (ortho-H of benzene rings) and the peak at 8.856 (8H of four pyrrole rings of ZnPP). The bonding degree (%) of ZnPP in ZnPP/PS sample was calculated with atomic absorption spectroscopy (AAS). By varying the used amount of $SnCl_4$ and the reaction temperature, the effects of these factors on the bonding reaction were examined to optimize it.

Researching Optical Properties of ZnPP/PS

Determination of electronic absorption spectrum: Solutions about $1.0 \times 10^{-6}M$ (concentration of ZnPP moieties) in ZnPP/PS without and with TBA were firstly prepared in DMF, respectively. Subsequently their electronic absorption spectra in the range of ultraviolet and visible light were determined.

For fluorescence studies, various concentrations (ranging from 0 to 0.3M) of TBA in the ZnPP/PS solutions were produced by dissolving appropriate amounts of TBA in measured volumes of solution, where the concentration of ZnPP moieties in these solutions was controlled at an order of magnitude of 10^{-6}mol/L to avoid the concentration quenching of ZnPP. Then the emission spectra of the above solutions were recorded by a fluorescence spectrometer. The instrument parameters were: excitation wavelength was set at 423 nm; excitation and emission slits were set at 5 nm band pass with a resolution of 1 nm.

The Stern–Volmer equation [eq. (1)] was used for the analysis of fluorescence quenching by an external quencher[32,33]:

$$\frac{F_0}{F} = 1 + K_Q[Q] \quad (1)$$

Where F_0 and F are quencher fluorescence intensities in the absence/presence of the quencher Q and K_Q is the Stern–Volmer quenching constant.

RESULTS AND DISCUSSION

Process to Prepare ZnPP/PS

In the presence of Lewis acid, the Friedel–Crafts alkylation reaction between the peripheral benzene ring around the porphyrin ring of ZnPP and the chloromethyl in the CMPS can be performed successfully under the appropriate reaction conditions, leading to the ZnPP/PS. The reaction process to prepare ZnPP/PS is schematically expressed in Scheme 1.

IR Spectra

Figure 1 gives the IR spectra of CMPS and ZnPP/PS. In the spectrum of CMPS, not only the main characteristic absorptions of benzene ring are displayed, but also the characteristic absorptions of chloromethyl groups are shown clearly, such as the vibration absorption of C—H at 1416 cm^{-1} and absorption of C—Cl at 676 cm^{-1} in -CH_2Cl. After ZnPP is bonded onto CMPS, the IR spectrum of ZnPP/PS is obviously different from that of CMPS. In the IR spectrum of ZnPP/PS, in addition to

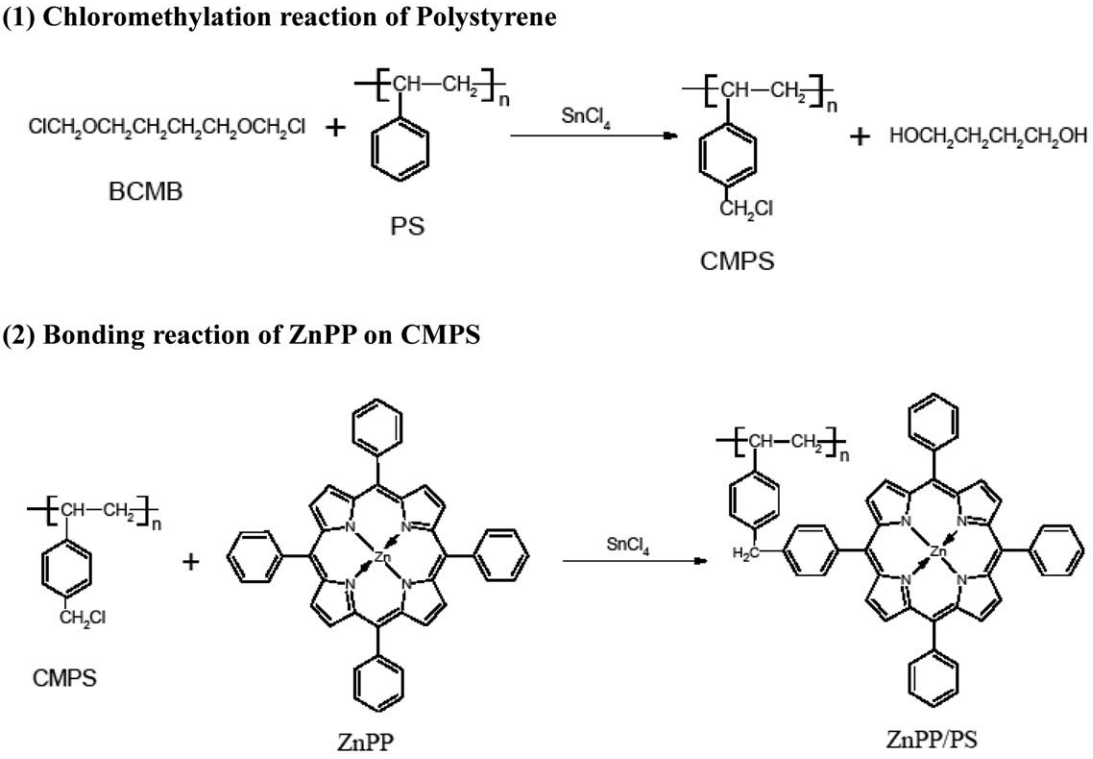

Scheme 1. Schematic express of preparing procedures for Zn porphyrin-functionalized polystyrene.

those above characteristic absorption bands of CMPS, the characteristic absorption bands of ZnPP also appear at 1352, 792, and 996 cm^{-1}, which correspond to the vibration of C═N in porphyrin ring, the skeletal vibration of porphyrin ring, and the vibration of N—Zn in ZnPP, respectively. Moreover, the characteristic absorptions of chloromethyl groups lessen greatly. The above spectra variations confirm fully the successful attachment of ZnPP moieties to the polymer matrix, i.e., obtaining the ZnPP/PS.

Effect of Various Factors on the Bonding Degree of ZnPP on ZnPP/PS

Temperature. Figure 2 shows the varying curves of the bonding degree of ZnPP with the reaction temperature. The Friedel–Crafts alkylation reaction is an exothermic chemical reaction,[34] and the effect of temperature on it is reflected in Figure 2 typically. It is indicated clearly from Figure 2 that the bonding degree of ZnPP rapidly increases with the rising temperature in the range 0–25°C, implying a heightened reaction rate, which is caused by dynamic features. But the bonding degree of ZnPP falls as the temperature is over than 25°C, which is governed mostly by thermodynamics. For the exothermic reaction, in consequence of its rise in temperature the equilibrium conversions of reactants decreases, leading to the decrease of bonding degree of ZnPP with a raised temperature ranged from

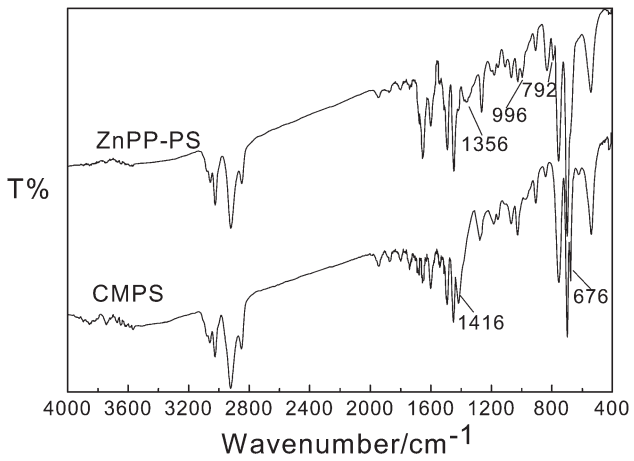

Figure 1. FTIR spectra of CMPS and ZnPP/PS.

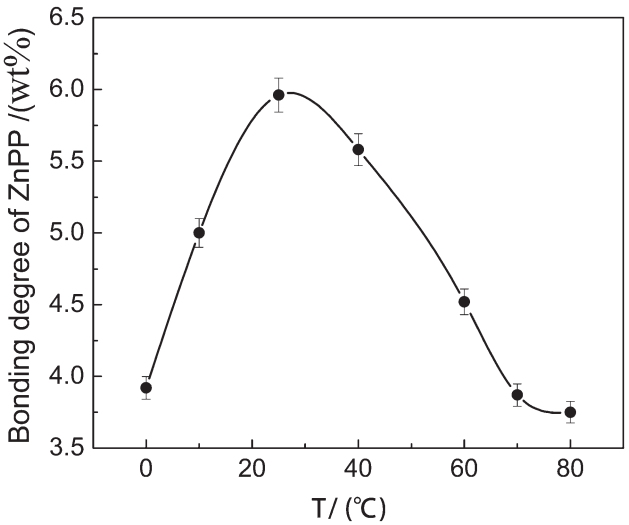

Figure 2. Variation of bonding degree of ZnPP with temperature. Amount of $SnCl_4$: 0.2 mL; Time: 8 h.

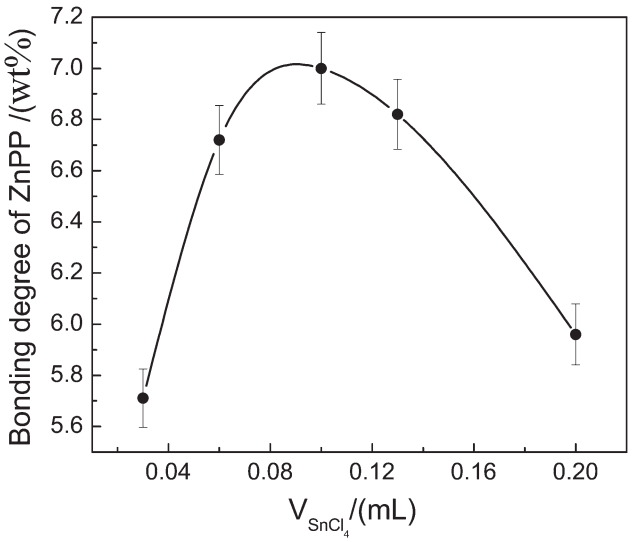

Figure 3. Variation of bonding degree of ZnPP with the amount of $SnCl_4$. Temperature: 25°C; Time: 8 h.

25 to 80°C. As a result of interaction of both dynamics and thermodynamics, the suitable temperature is determined to be 25°C finally.

The Amount of Catalyst. The bonding reaction of ZnPP on CMPS was performed in DMF using $SnCl_4$ as the catalyst. Figure 3 shows the bonding degree (wt %) of ZnPP on PS as a function of the amount of $SnCl_4$. It could be observed distinctly from Figure 3 that the bonding degree of ZnPP increases at first with the increasing amount of $SnCl_4$, and then decreases. This is because the increase of $SnCl_4$ would accelerate the reaction between ZnPP and chloromethyl, and promote the formation of carbonium ions, so that the rate of Friedel–Crafts alkylation reaction speeds up, leading to the higher bonding degree of ZnPP. However, as $SnCl_4$ is overdone, an awful lot of carbonium ions form quickly, which could react not only with peripheral benzene rings on ZnPP, but also with the benzene rings on other CMPS chains, making polymers cross-linked. Therefore, the greater steric hindrance occurs between ZnPP and CMPS, and the effective reactive sites lessen for the Friedel–Crafts alkylation reaction. Finally, the bonding degree of ZnPP decreases reversely whereas the amount of $SnCl_4$ is more than 0.1 mL. Due to all the reasons mentioned above, the optimal amount of $SnCl_4$ should be 0.1 mL to gain the higher bonding degree of ZnPP and the linear objects ZnPP/PS.

Electronic Absorption Spectra

Figure 4 shows the absorption spectra of ZnPP/PS solution in the absence and presence of TBA in DMF. For porphyrins, there are two energy levels with adjacent energy on HOMO orbital, $a_{1\mu}(\pi)$ and $a_{2\mu}(\pi)$, and there is a pair of degenerate energy levels, $e_g(\pi^*)$, on LUMO orbital. In the spectrum of ZnPP/PS, the intensive band at 423 nm belongs to Soret band arising from the transition of $a_{1\mu}(\pi) \rightarrow e_g(\pi^*)$, and the intensities of other two bands at 559 and 599 nm are low and these bands are assigned to Q-bands corresponding to the transition of of $a_{2\mu}(\pi) \rightarrow e_g(\pi^*)$. The shape of the spectrum and the band positions are in accordance with that of ZnPP in the literature,[26] which indicates the existence of ZnPP in PS. So the ZnPP/PS possesses the characteristic electronic absorption spectrum of the free ZnPP.

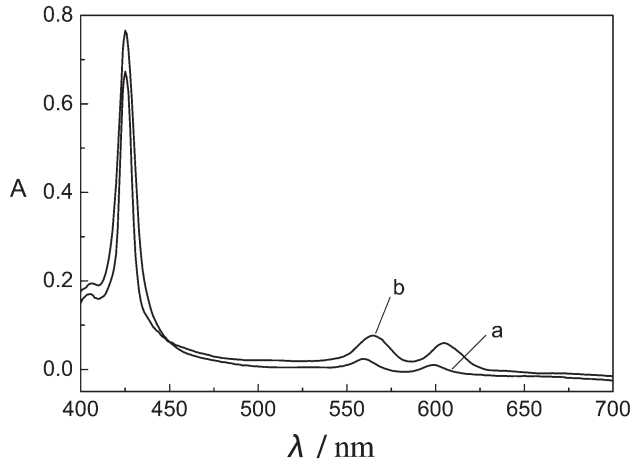

Figure 4. Electronic absorption spectra of ZnPP/PS with and without TBA in DMF (a) without TBA; (b) with TBA.

After adding TBA into ZnPP/PS, the variation of electronic absorption spectrum is shown in Figure 4. It can be seen that the absorption peak of Q-band of ZnPP/PS with TBA shows an obvious red shift compared with that of ZnPP/PS without TBA, which is closely connected to the narrower LUMO–HOMO energy gap mainly resulted from the formation of metal–ligand bond between ZnPP moieties in ZnPP/PS and TBA (Scheme 2).[35] The N atoms on triazine ring of TBA are electron-rich. When metal–ligand bond between ZnPP and TBA is formed, portion of the charge of the N atom of TBA will transfer to the porphyrin ring through the zinc ion, so that the electron density of the porphyrin ring increases, and the LUMO-HOMO energy gap reduces, leading to the red shift of absorption peaks.

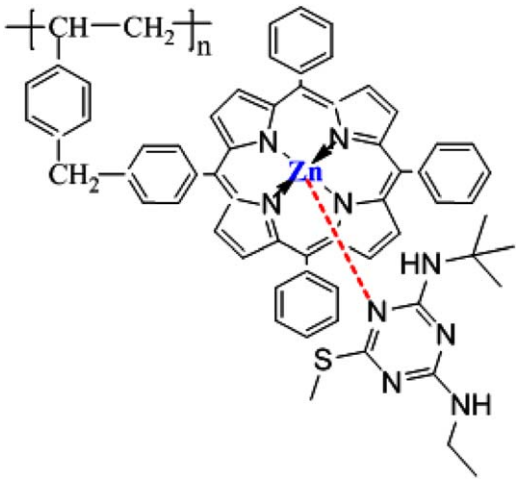

Scheme 2. Schematic illustration of a possible mechanism between ZnPP/PS and TBA. [Color figure can be viewed in the online issue, which is available at wileyonlinelibrary.com.]

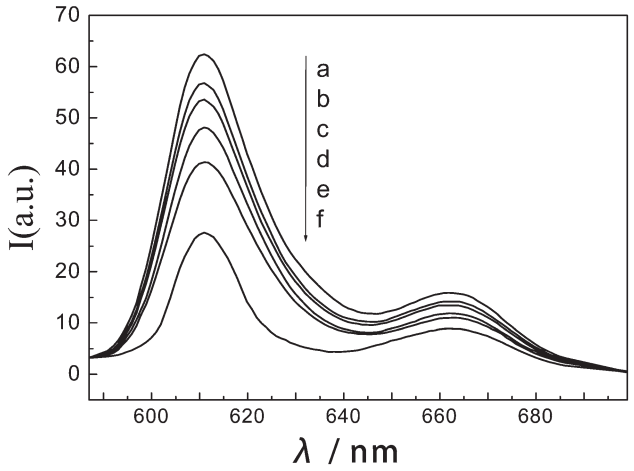

Figure 5. Fluorescence emission spectra of ZnPP/PS at 423 nm excitation wavelength with: (a) no TBA, (b) 0.001*M*, (c) 0.004*M*, (d) 0.01*M*, (e) 0.04*M*, (f) 0.1*M* of TBA.

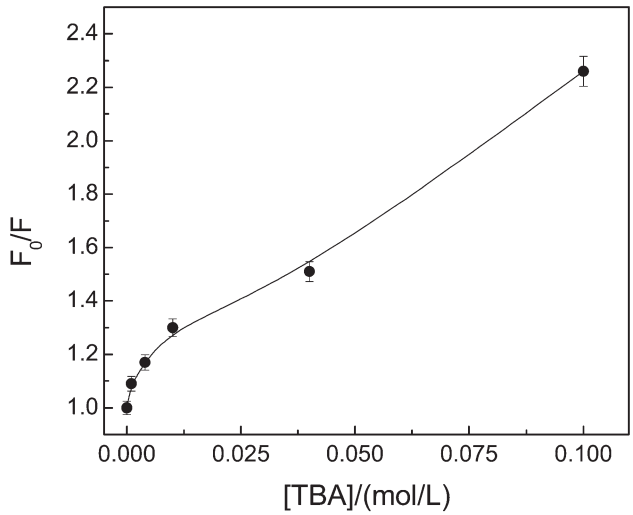

Figure 7. A Stern–Volmer-type plot for the TBA quenching of ZnPP/PS in DMF.

Fluorescence Quenching of ZnPP/PS by TBA

The fluorescence emission spectra of ZnPP/PS in the absence and presence of TBA with an identical ZnPP concentration of (1.00×10^{-6} mol·L^{-1}) were measured with an excitation wave at 423 nm, and were shown in Figure 5. It can be found in Figure 5 that ZnPP/PS shows the intensive fluorescence and the spectrum exhibits two bands in the range of 580–700 nm, which originate from the jump of $S_1 \rightarrow S_0$ (from the first excited state to the ground state). As they are corresponding to the Q-band in the adsorption spectrum, so called the Q-emission band. The emission spectrum of ZnPP/PS is basically agreement with the free ZnPP in the literature,[26] indicating again that ZnPP is attached to the polymer matrix successfully and ZnPP/PS gained possesses the characteristic fluorescence spectrum of the free ZnPP. Moreover, the fluorescence intensity decreases upon the successive addition of TBA (Figure 5), i.e., TBA quenches ZnPP/PS emission intensity. In our case, we can neglect concentration quenching by the ZnPP/PS because of the low concentration used and the absence of ZnPP aggregates. As seen in Figure 6, the concentration quenching by the ZnPP/PS would take place while the concentration of ZnPP moieties in the ZnPP/PS polymer matrix is over than 1.00×10^{-6} mol/L. Fluorescence quenching can still occur by dynamic quenching (collisional quenching), static quenching, or by combined dynamic and static quenching mechanisms.[33] Fluorescence quenching data, obtained with TBA as the external quencher of fluorescence of ZnPP/PS, were analyzed using the Stern–Volmer equation [eq. (1)], and the data are interpreted by plotting F_0/F versus [TBA] graph. According to the quenching mechanism, the ZnPP emission intensity quenched by TBA is either by dynamic or static quenching process when Stern–Volmer plot is linear; dynamic quenching process affects the excited states of the fluorophore, and for this reason the adsorption spectra are not expected to change during dynamic quenching[36]; but in

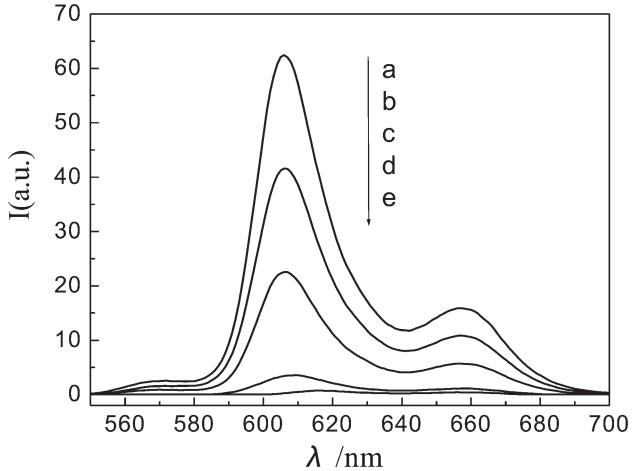

Figure 6. Fluorescence emission spectra of ZnPP/PS with various concentrations of ZnPP moieties (a) 1.00×10^{-6}*M*, (b) 5.00×10^{-6}*M*, (c) 2.00×10^{-7}*M*, (d) 2.00×10^{-5}*M*, (e) 8.32×10^{-5}*M*.

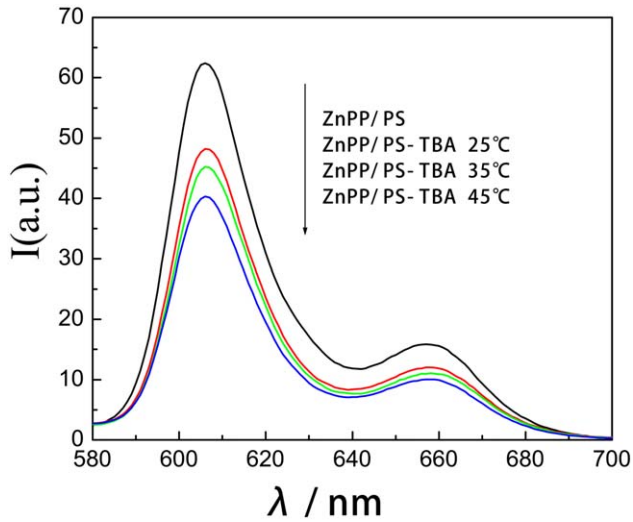

Figure 8. Fluorescence emission spectra of ZnPP/PS without TBA and ZnPP/PS with 0.01*M* of TBA at different temperatures. [Color figure can be viewed in the online issue, which is available at wileyonlinelibrary.com.]

static quenching where a complex is formed in the ground state, changes in the adsorption spectrum of the fluorophore are expected;[19] this is not observed (cf. Figure 7).

In addition, a fluorophore can be quenched both by collision and by complex formation with the same quencher,[33] and the plot of F_0/F versus $[Q]$ for this combined dynamic and static process would yield a non-linear graph; this is shown in Figure 7. It is because some of TBA interacts with ZnPP moieties in the ZnPP/PS polymer matrix to make a single (TBA–ZnPP/PS) complex in the ground state with an adsorption spectrum different than that of ZnPP/PS alone (cf. Figure 4), which shows the static quenching process; at the mean time, some other quencher TBA could diffuse to ZnPP moieties during the lifetime of excited state of ZnPP for the larger TBA concentration, and the fluorophore returns to the ground state without emission of a photon. Figure 8 gives the fluorescence emission spectra of ZnPP/PS in the absence and presence of TBA with an identical ZnPP concentration of (1.00×10^{-6} mol·L^{-1}) at different temperatures with the excitation wave of 423 nm. It is seen in Figure 8 that the higher the temperature, the more the fluorescence quenching of ZnPP/PS by TBA, which shows that the dynamic quenching process occurs.[33] As a result, the non-linear Stern–Volmer plot indicates the combined dynamic and static quenching of ZnPP/PS by TBA.

CONCLUSIONS

The data presented in this work confirm the successful attachment of ZnPP to PS matrix, the strong the characteristic spectra of ZnPP/PS similar to ZnPP, and an interaction between TBA and ZnPP/PS that changes both the absorbance and fluorescence characteristics of the porphyrin. The variety in absorbance spectrum indicates the formation of the complexes between TBA and ZnPP/PS in the ground state. As for the fluorescence quenching of ZnPP/PS by TBA, the plot of F_0/F versus [TBA] demonstrates that TBA doesn't only interact with ZnPP/PS in the ground state to form a non-fluorescent complex, but also likely diffuse to ZnPP moieties during the lifetime of excited state of ZnPP/PS. In other words, the quenching mechanism of ZnPP/PS by TBA is due to the combined dynamic and static quenching process. These changes in the spectrophotometric characteristics of ZnPP/PS could be used for the detection and quantification of TBA in the environmental water.

ACKNOWLEDGMENTS

The authors gratefully acknowledge the National Science Foundation of China (No. 21307116) and the Youth Science and Technology Foundation of province Shanxi of China (No. 2010021008-4) for financial support of this work.

REFERENCES

1. Zhao, G. Y.; Song, S. J.; Wang, C.; Wu, Q. H.; Wang, Z. *Anal. Chim. Acta* **2011**, *708*, 155.
2. Wu, Q. H.; Li, Z.; Wu, C. X.; Wang, C.; Wang, Z. *Microchim. Acta* **2010**, *170*, 59.
3. Wang, H.; Li, G. J.; Zhang, Y. Q.; Chen, H. Y.; Zhao, Q.; Song, W. T.; Xu, Y.; Jin, H. Y.; Ding, L. *J. Chromatogr. A* **2012**, *1233*, 36.
4. Shen, G.; Lee, H. K. *J. Chromatogr. A* **2003**, *985*, 167.
5. Baranowska, I.; Barchanska, H.; Pacak, E. *Environ. Pollut.* **2006**, *143*, 206.
6. See, H. H.; Sanagi, M. M.; Ibrahim, W. A. W.; Naim, A. A. *J. Chromatogr. A* **2010**, *1217*, 1767.
7. Sanagi, M. M.; Abbas, H. H.; Ibrahim, W. A. W.; Aboul-Enien, H. Y. *Food Chem.* **2012**, *133*, 557.
8. Li, H. F.; Xie, C. G.; Li, S. Q.; Xu, K. *Colloids Surf. B* **2012**, *89*, 175.
9. Lefèvre, F.; Chalifour, A.; Yu, L. P.; Chodavarapu, V.; Juneau, P.; Izquierdo, R. *Lab Chip* **2012**, *12*, 787.
10. Santos, C. I. M.; Oliveira, E.; Barata, J. F. B.; Faustino M. A. F.; Cavaleiro, J. A. S.; Neves, M. G. P. M. S.; Lodeiro, C. *J. Mater. Chem.* **2012**, *22*, 13811.
11. Kim, Y. J.; Seong, D.Y. *J. Mater. Sci.* **2013**, *48*, 3486.
12. Seong, D. Y.; Choi, M. S.; Kim, Y. J. *Eur. Polym. J.* **2012**, *48*, 1988.
13. Li, Y.; Bian, Y.; Yan, M.; Thapaliya, P. S.; Johns, D.; Yan, X.; Galipeau, D.; Jiang, J. *J. Mater. Chem.* **2011**, *21*, 11131.
14. Li, Y.; Lu, P.; Yan, X.; Jin, L.; Peng, Z. *RSC Adv.* **2013**, *3*, 545.
15. Xiang, N.; Liu, Y. J.; Zhou, W. P.; Huang, H. P.; Guo, X. P.; Tan, Z. P.; Zhao, B. P.; Shen, P.; Tan, S. T. *Eur. Polym. J.* **2010**, *46*, 1084.
16. Thomas, A. P.; Babu, P. S. S.; Nair, S. A.; Ramakrishnan, S.; Ramaiah, D.; Chandrashekar, T. K.; Srinivasan, A.; Pillai, M. R. *J. Med. Chem.* **2012**, *55*, 5110.
17. Zhang, J. F.; Zhou, Y.; Yoon, J. Y.; Kim, Y. M.; Kim, J. S. *Org. Lett.* **2010**, *12*, 3852.
18. Okamoto, K.; Fukuzumi, S. *J. Am. Chem. Soc.* **2004**, *126*, 13922.
19. Rahman, M.; Harmon, H. *J. Spectrochim. Acta A* **2006**, *65*, 901.
20. Schneider, H. J.; Wang, M. *J. Org. Chem.* **1994**, *59*, 7464.
21. Chen, Y. T.; Jiang, J. Z. *Org. Biomol. Chem.* **2012**, *10*, 4782.
22. Nardis, S.; Pomarico, G.; Tortora, L.; Capuano, R.; D'Amico, A.; Natale, C. D.; Paolesse, R. *J. Mater. Chem.* **2011**, *21*, 18638.
23. Whittington, C. L.; Maza, W. A.; Woodcock, H. L.; Larsen, R. W. *Inorg. Chem.* **2012**, *51*, 4756.
24. Matsui, J.; Higashi, M.; Takeuchi, T. *J. Am. Chem. Soc.* **2000**, *122*, 5218.
25. Wang, R. X.; Jiao, W. Z.; Gao, B. *J. Polym. Advan. Technol.* **2010**, *21*, 447.
26. Wang, R. X.; Gao, B. J.; Wang, F. Y. *Acta Polym. Sin.* **2009**, *11*, 1113.
27. Silva, M.; Azenha, M. E.; Pereira, M. M.; Burrows, H. D.; Sarakha, M.; Forano, C.; Ribeiro, M. F.; Fernandes, A. *Appl. Catal. B* **2010**, *100*, 1.
28. Bartelmess, J.; Soares, A. R. M.; Martínez-Díaz, M. V.; Neves, M. G. P. M. S.; Tomé, A. C.; Cavaleiro, J. A. S.; Torres, T.; Guldi, D. M. *Chem. Commun.* **2011**, *47*, 3490.

29. Wang, R. X.; Jiao, W. Z.; Gao, B. *J. Appl. Surf. Sci.* **2010**, *256*, 3031.

30. Wang, R. X.; Gao, B. J.; Jiao, W. Z. *Appl. Surf. Sci.* **2009**, *255*, 4109.

31. Shen, Y. L.; Yang, Y. F.; Gao, B. J.; Zhu, Y. *Acta Polym. Sin.* **2007**, *6*, 559.

32. Moan, J.; Kvam, E.; Hoving, E.; Berg, K. In Effects of PDT on DNA and Chromosomes. Photobiology, Riklis, E. Ed.; Plenum Press: New York, **1991**.

33. Lakowicz, J. R. Principles of Fluorescence Spectrocopy, 2nd ed.; Kluwer Academic/Plenum: New York, **1999**.

34. Hu, Y. F.; Lin, G. Q. Modern Organic Reactions–Metal Catalyzed Reactions, Vol. *5*, Chemical Industry Press: Beijing, **2008**; p 54.

35. Huang, C. Y.; Yeh, W. L.; Cheng, S. H. *J. Electroanal. Chem.* **2005**, *577*, 179.

36. Wróbel, D.; Łukasiewicz, J.; Manikowski, H. *Dyes Pigments* **2003**, *58*, 7.